Biceps Pulley Lesions: Diagnostic Accuracy of Nonarthrographic Shoulder MRI and the Value of Various Diagnostic Signs

Mohamad Gamal Nada, MD,[1] Yassir Edrees Almalki, MD,[2,3] Mohammad Abd Alkhalik Basha, MD,[1*] Yasmin Ibrahim Libda, MD,[1] Mohamed M. A. Zaitoun, MD,[1] Ahmed A. El-Hamid M. Abdalla, MD,[1] Rania Mostafa Almolla, MD,[1] Hanan A. Hassan, MD,[1] Tamer Mahmoud Dawoud, MD,[4] Ahmad Hassan Zaki Eissa, MD,[5] Sharifa Khalid Alduraibi, MD,[6] Diaa Bakry Eldib, MD,[7] and Yara Mohammed Ahmad Ali Ziada, MD[8]

Background: There is limited data in the literature regarding the role of nonarthrographic MRI for detecting biceps pulley (BP) lesions.
Purpose: To assess the accuracy of nonarthrographic MRI for detecting BP lesions, and to evaluate the diagnostic value of various MRI signs (superior glenohumeral ligament discontinuity/nonvisibility, long head of biceps (LHB) displacement sign or subluxation/dislocation, LHB tendinopathy, and supraspinatus and subscapularis tendon lesions) in detecting such lesions.
Study Type: Retrospective.
Population: 84 patients (32 in BP-lesion group and 52 in BP-intact group-as confirmed by arthroscopy).
Field Strength/Sequence: 1.5-T, T1-weighted turbo spin echo (TSE), T2-weighted TSE, and proton density-weighted TSE spectral attenuated inversion recovery (SPAIR) sequences.
Assessment: Three radiologists independently reviewed all MRI data for the presence of BP lesions and various MRI signs. The MRI signs and final MRI diagnoses were tested for accuracy regarding detecting BP lesions using arthroscopy results as the reference standard. Furthermore, the inter-reader agreement (IRA) between radiologists was determined.
Statistical Tests: Student's *t*-tests, Chi-squared, and Fisher's exact tests, and 4-fold table test were used. The IRA was calculated using Kappa statistics. A *P*-value <0.05 was considered statistically significant.
Results: The sensitivity, specificity, and accuracy of nonarthrographic MRI for detecting BP lesions were 65.6%–78.1%, 90.4%–92.3%, and 81%–86.9%, respectively. The highest accuracy was noticed for the LHB displacement sign (84.5%–86.9%), and the highest sensitivity was registered for the LHB tendinopathy sign (87.5%). Furthermore, the highest specificity was observed for the LHB displacement sign and LHB subluxation/dislocation sign (98.1%–100%). The IRA regarding final MRI diagnosis and MRI signs of BP lesions was good to very good ($\kappa = 0.76$–0.98).
Data Conclusion: Nonarthrographic shoulder MRI may show good diagnostic accuracy for detecting BP lesions. The LHB displacement sign could serve as the most accurate and specific sign for diagnosis of BP lesions.
Level of Evidence: 3
Technical Efficacy: Stage 2

J. MAGN. RESON. IMAGING 2023.

View this article online at wileyonlinelibrary.com. DOI: 10.1002/jmri.29004

Received May 28, 2023, Accepted for publication Jul 7, 2023.

*Address reprint requests to: M.A.A.B., Assistant Professor of Radiodiagnosis, Faculty of Human Medicine, Zagazig University, Zagazig, Egypt.
E-mail: mohammad_basha76@yahoo.com

From the [1]Department of Radiology, Faculty of Human Medicine, Zagazig University, Zagazig, Egypt; [2]Division of Radiology, Medical College, Najran University, Najran, Kingdom of Saudi Arabia; [3]Department of Internal Medicine, Medical College, Najran University, Najran, Kingdom of Saudi Arabia; [4]Department of Diagnostic Radiology, Faculty of Human Medicine, Tanta University, Tanta, Egypt; [5]Department of Orthopedic Surgery and Traumatology, Faculty of Human Medicine, Zagazig University, Zagazig, Egypt; [6]Department of Radiology, College of Medicine, Qassim University, Buraidah, Kingdom of Saudi Arabia; [7]Department of Radiology, Faculty of Human Medicine, Benha University, Benha, Egypt; and [8]Department of Radiology, General Organization for Teaching Hospitals and Medical Institutes (GOTHI), Al-Ahrar Teaching Hospital, Zagazig, Egypt

Biceps pulley (BP) lesions are often referred to as hidden lesions because of the difficulty in clinical and arthroscopic identification.[1] The BP structures, also known as the biceps-anchoring apparatus, stabilize the reflected part of the long head of the biceps (LHB) tendon as it curves intra-articularly from its origin at the supraglenoid tubercle and along its course to the bicipital groove.[2] These structures are the superior glenohumeral ligament (SGHL), the coracohumeral ligament (CHL), the supraspinatus (SSP) tendon, and the subscapularis (SSC) tendon.[1–4] Overall, BP lesions are not uncommon, with an arthroscopic prevalence of ~7%.[5] Furthermore, BP lesions can be congenital, traumatic, degenerative, or occur secondary to injury to the surrounding structures.[1] Those lesions can result in persistent anterior shoulder pain and LHB instability (subluxation or dislocation), which in turn may successively induce rotator cuff tendon lesions and anterosuperior shoulder impingement if left untreated.[2,6] Several classifications have been published for BP lesions and the associated LHB instability.[5–8] Currently, the Habermeyer classification is widely used to classify BP lesions as isolated SGHL tears (Group I), SGHL and SSP tendon tears (Group II), SGHL and SSC tendon tears (Group III), or SGHL, SSP tendon, and SSC tears (Group IV).[7]

The difficulty in the clinical and arthroscopic detection of BP lesions highlights the relevance of imaging assessment.[9] In this context, MR arthrography (MRA) has been found to be the best imaging modality for illustrating the normal anatomy of the pulley apparatus and identifying BP lesions.[10] Because the BP is composed of several small anatomic structures that lie very close to one another and blend together at their distal attachment sites, the nonarthrographic MRI can be challenging to evaluate.[1] However, many centers lack the capability for intra-articular contrast injection.

Nonarthrographic shoulder MRI is routinely performed for the assessment of different shoulder pathologies. Despite the advantages of MRI, such as high soft-tissue resolution and noninvasiveness, few studies have investigated the diagnostic accuracy of nonarthrographic MRI in detecting BP lesions and LHB instability.[11–13] Therefore, we aimed to assess the diagnostic accuracy of nonarthrographic shoulder MRI for detecting BP lesions, using arthroscopy results as the reference standard. We also aimed to assess the diagnostic value of MRI signs for BP lesions to avoid missing hidden lesions and enable early and suitable management.

Materials and Methods

This retrospective cross-sectional study was approved by the institutional review board (approval number: ZU-IRB# 9857; approved on September 26, 2022). The requirement for written informed consent was waived due to the retrospective design of this study. All procedures were conducted according to the principles expressed in the Declaration of Helsinki.

Study Population

This study included all patients who underwent shoulder MRI with subsequent shoulder arthroscopy at our institution between September 2020 and December 2022. Initially, the search resulted in a total of 244 patients. All MRI examinations and arthroscopic reports were retrieved. Patients younger than 16 years ($n = 2$), patients with previous shoulder surgeries ($n = 62$), patients with adhesive capsulitis ($n = 21$), patients with arthroscopic reports lacking full comments about BP structures ($n = 28$), and MRI examinations performed at other institutions with different MRI protocols ($n = 47$) were excluded from the study. The exclusion criteria resulted in a final cohort of 84 eligible patients (52 males and 32 females; age range: 24–69 years). The flowchart of the study is illustrated in Fig. 1. The mean age in the BP-lesion group was 43.4 ± 11.3 years, and in the BP-intact group it was 44.8 ± 10.3 years. The BP-lesion group included 18 right and 14 left shoulders, whereas the BP-intact group included 31 right and 21 left shoulders.

MRI Protocol

All MRI scans were performed at our musculoskeletal MRI unit using a 1.5-T scanner (Achieva, Philips Medical Systems, Best, The Netherlands) and a dedicated shoulder coil (dS Shoulder 8ch 1.5T Invivo Corporation, USA). Patients were placed in a neutral position with external rotation. The protocol included three plane localizers: 1) axial T1-weighted turbo spin echo (TSE) sequences (repetition time [TR] = 646 msec, echo time [TE] = 10 msec) and proton density-weighted (PDW) TSE spectral attenuated inversion recovery (SPAIR) sequences (TR = 2500 msec, TE = 25 msec); 2) coronal oblique T1-weighted TSE (TR = 450 msec, TE = 10 msec), T2-weighted TSE (TR = 3200 msec, TE = 80 msec), and PDW TSE SPAIR sequences (TR = 2500 msec, TE = 25 msec); and 3) sagittal oblique PDW TSE SPAIR (TR = 2500 msec, TE = 25 msec) ± T2-weighted TSE sequences (TR = 3333 msec, TE = 80 msec). The field of view was 140–180 mm, the section thickness was 3 mm, and the intersection gap was 0.3 mm.

Image Analysis

Three radiologists (M.A.A.B., Y.M.A.A.Z., and M.G.N. with 16, 12, and 10 years of experience in musculoskeletal MRI, respectively) independently, and in a blinded fashion, reviewed all MRI data using the picture archiving and communication system (PACS; PaxeraUltima, Paxera Viewer version 5.0.9.6, PaxeraHealth, Newtone, MA, USA). Clinical data and arthroscopic reports were concealed from the radiologists. The images were assessed for the presence of BP lesions defined by SGHL discontinuity or non-visibility, the LHB tendon displacement sign, or LHB tendon subluxation or dislocation. The LHB tendon displacement sign was evaluated on sagittal oblique images of the lesser humeral tuberosity. Any LHB tendon subluxation or dislocation was assessed on the axial images in relation to the bicipital groove. Furthermore, the images were assessed for LHB tendinopathy, and SSP and SSC tendon lesions. Finally, the radiologists evaluated all MRI signs (Fig. 2)[14] for each patient and assigned a final MRI diagnosis of the BP lesion as positive or negative based on subjective assessment. The MRI signs and the final MRI diagnosis were tested for their performance in detecting BP lesions, using arthroscopy results as the

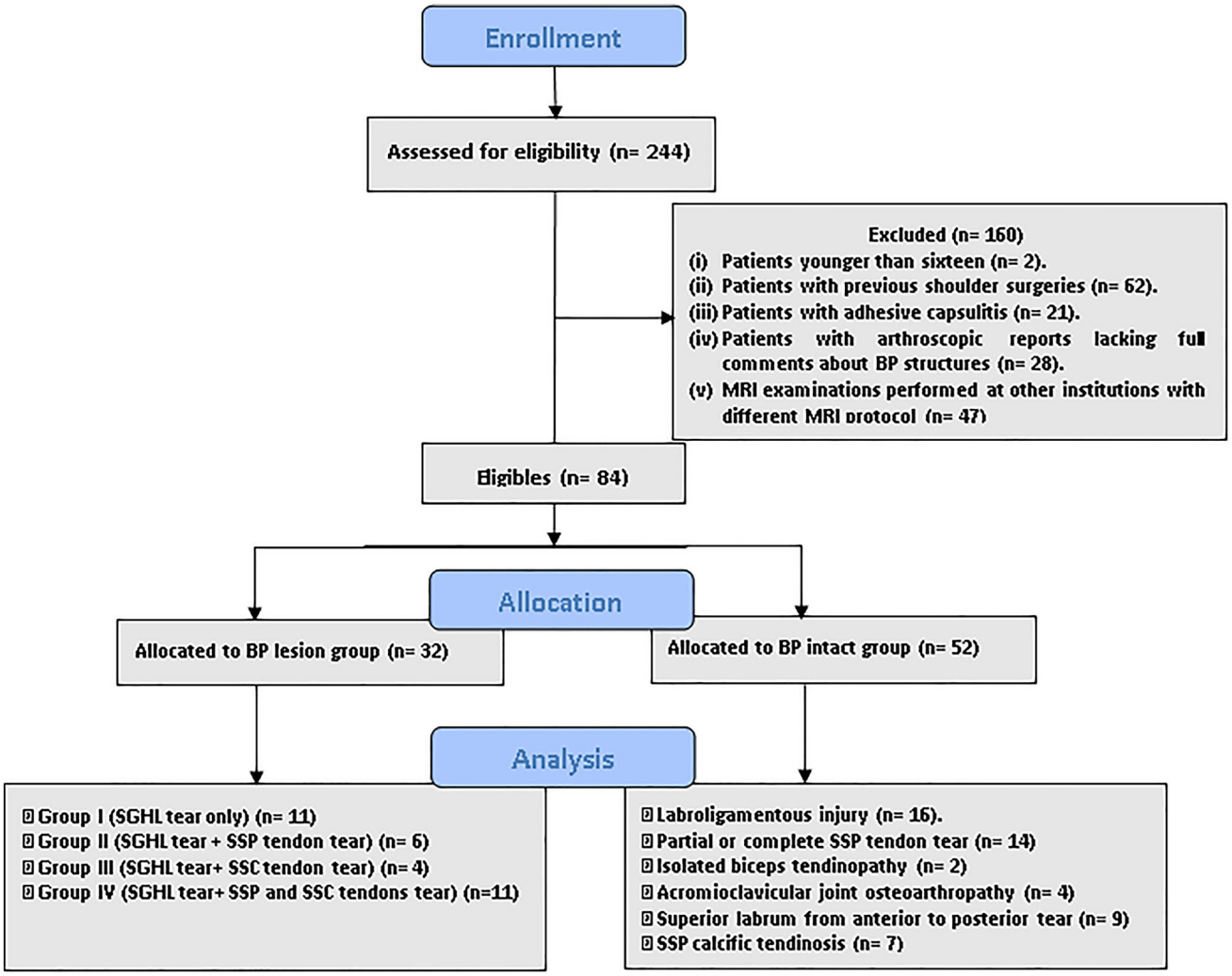

FIGURE 1: Flow chart of the study.

reference standard. Inter-reader agreement (IRA) was determined between the radiologists concerning the MRI signs and the final MRI diagnosis of BP lesions.

Arthroscopy

All arthroscopic procedures were performed within 1 month of MRI examination. Two consultants in orthopedic surgery with 16 years of

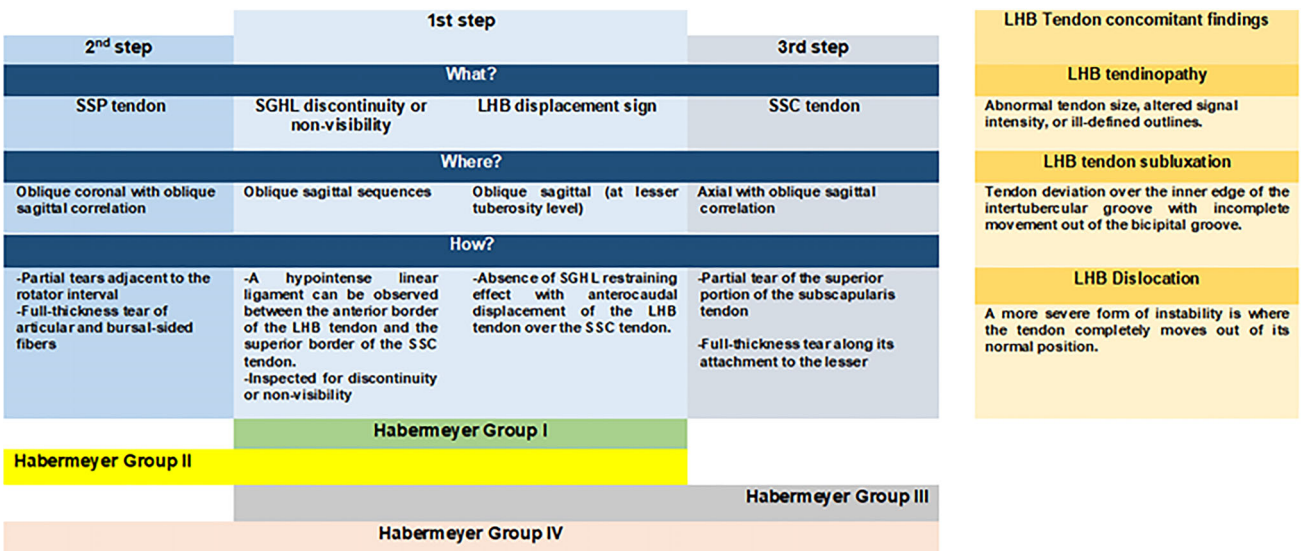

FIGURE 2: Diagram describes the steps and diagnostic criteria for various MRI signs of BP lesions.

shoulder arthroscopy experience performed all procedures. All surgeons were aware of the MRI reports. Each arthroscopic report was retrospectively evaluated for full comment on the integrity of the biceps tendon and its anchoring apparatus structures (SGHL, SSP, and SSC tendons). Based on arthroscopic findings, the patients were divided into two groups. Group A (BP-lesion group) included patients with positive arthroscopic results for BP lesions and were classified according to the criteria of Habermeyer et al.[7] Group B (BP-intact group) included patients with negative arthroscopic results for the BP lesions. Arthroscopic reports were used as the reference standard for the final diagnosis of the BP lesions.

Statistical Analysis

MedCalc statistical software (version 20.022; Ostend, Belgium) was used for statistical analysis. Categorical data are presented as numbers and percentages. The two groups were compared using the Chi-squared or Fisher's exact tests. The standard deviation, mean, median, and range are used for quantitative data. The normally distributed quantitative variables of the two groups were compared using the student's *t*-test. The 4-fold table test was used to calculate the diagnostic accuracy of nonarthrographic MRI and the MRI signs for detecting BP lesions, using arthroscopy results as the reference standard. The IRA for the MRI signs and the final MRI diagnosis was calculated using the Kappa statistics. The values obtained were interpreted as follows: 0.00–0.20, poor agreement; 0.21–0.40, fair agreement; 0.41–0.60, moderate agreement; 0.61–0.80, good agreement; and 0.81–1.00, very good agreement. A *P*-value <0.05 was considered statistically significant.

Results

Arthroscopic Findings

Based on the arthroscopic findings, the BP-lesion group included 32 patients, and the BP-intact group included 52 patients. The final arthroscopic grading of the BP lesions was as follows: Group I (11/32; 34.4%), Group II (6/32; 18.8%), Group III (4/23; 12.5%), and Group IV (11/32; 34.4%). The final arthroscopic diagnoses in the BP-intact group were as follows: labroligamentous injury (16/52), partial or complete SSP tendon tear (14/52), isolated biceps tendinopathy (2/52), acromioclavicular joint osteoarthropathy (4/52), superior labrum from anterior to posterior tear (SLAP) (9/52), and SSP calcific tendinosis (7/52).

Findings from MRI

Table 1 shows the MRI findings. According to the image readers, LHB tendinopathy was the most frequently diagnosed sign in the BP-lesion group (87.5%), followed by SGHL discontinuity or the nonvisibility sign (56.3%–68.8%) and LHB displacement sign (59.4%–65.6%). Furthermore, LHB subluxation or dislocation was the least frequently diagnosed sign in the BP-lesion group (37.5%–43.8%). Additionally, SSP tendon lesions were noticed in 65.3%–59.4% of patients in the BP-lesion group, and SSC tendon lesions were noticed in 46.9%–50.0% of patients in the BP-lesion group. Moreover, SSP tendon lesions were the most frequently misdiagnosed sign in the BP-intact group (25%), followed by LHB tendinopathy (19.2%–21.2%).

TABLE 1. Nonarthrographic Shoulder MRI Findings

MRI signs	BP-lesion group ($n = 32$)	BP-intact group ($n = 52$)
SGHL discontinuity/ nonvisibility		
Reviewer 1	20 (62.5)	4 (7.7)
Reviewer 2	18 (56.3)	5 (9.6)
Reviewer 3	22 (68.8)	4 (7.7)
LHB displacement on sagittal images		
Reviewer 1	20 (65.6)	0 (0)
Reviewer 2	19 (59.4)	0 (0)
Reviewer 3	21 (65.6)	0 (0)
LHB subluxation/dislocation on axial images		
Reviewer 1	12 (37.5)	1 (1.9)
Reviewer 2	14 (43.8)	0 (0)
Reviewer 3	14 (43.8)	0 (0)
LHB tendinopathy		
Reviewer 1	28 (87.5)	11 (21.2)
Reviewer 2	28 (87.5)	10 (19.2)
Reviewer 3	28 (87.5)	11 (21.2)
SSP tendon lesion		
Reviewer 1	19 (59.4)	13 (25)
Reviewer 2	18 (56.3)	13 (25)
Reviewer 3	19 (59.4)	13 (25)
SSC tendon lesion		
Reviewer 1	15 (46.9)	5 (9.6)
Reviewer 2	16 (50.0)	3 (5.8)
Reviewer 3	16 (50.0)	3 (5.8)

Data represent number of lesions with percentage in parenthesis.
BP: biceps pulley; SGHL: superior glenohumeral ligament; LHB: long head of biceps; SSP: supraspinatus; SSC: subscapularis.

Diagnostic Accuracy of MRI

Using the results of arthroscopy as the reference standard, Table 2 summarizes the diagnostic accuracy of MRI for detecting BP lesions. According to the image readers, the

TABLE 2. Diagnostic Accuracy of Nonarthrographic Shoulder MRI in Detecting BP Lesions

Value	Reviewer 1	Reviewer 2	Reviewer 3
Sensitivity	75.0 (24/32) [56.6–88.5]	65.6 (21/32) [46.8–81.4]	78.1 (25/32) [60.0–90.7]
Specificity	92.3 (48/52) [81.5–97.8]	90.4 (47/52) [78.9–96.8]	92.3 (48/52) [81.5–97.8]
Accuracy	85.7 (72/84) [76.4–92.4]	81.0 (68/84) [70.9–88.7]	86.9 (73/84) [77.8–93.3]
PPV	85.7 (24/28) [69.6–94.0]	80.8 (21/26) [63.8–90.9]	86.2 (25/29) [70.5–94.2]
NPV	85.7 (48/56) [76.6–91.6]	81.0 (47/58) [72.4–87.4]	87.3 (48/55) [78.0–92.9]

Data in parentheses were used to calculate percentages. Data in brackets are 95% confidence intervals.
BP: biceps pulley; PPV: positive predictive value; NPV: negative predictive value.

sensitivity, specificity, and accuracy of MRI for detecting BP lesions were 65.6%–78.1%, 90.4%–92.3%, and 81%–86.9%, respectively.

Diagnostic Value of MRI Signs

As shown in Table 3, we evaluated the diagnostic value of various MRI signs for detecting BP lesions compared to arthroscopy findings. Based on the image readers' evaluations, the highest accuracy was noticed for the LHB displacement sign (84.5%–86.9%), the highest sensitivity was noticed for the LHB tendinopathy sign (87.5%), and the highest specificity was noticed for the LHB displacement sign and LHB subluxation or dislocation sign (98.1%–100%). The lowest accuracy was noticed for the SSP tendon lesion (67.9%–69.0%), the lowest sensitivity was noticed for the LHB subluxation or dislocation sign (37.5%–47.8%), and the lowest specificity was noticed for the SSP tendon lesion (75.0%).

Inter-Reader Agreement

The IRA for MRI signs and the final MRI diagnosis of BP lesions is listed in Table 4. The IRA regarding the final MRI diagnosis of the BP lesions was good ($\kappa = 0.78$). The IRA was good to very good regarding the various MRI signs ($\kappa = 0.76$–0.98). Examples of cases from our study are shown in Figs. 3–7.

Discussion

The current study demonstrated that nonarthrographic shoulder MRI is potentially highly accurate in detecting BP lesions with an overall sensitivity, specificity, and accuracy of 65.6%–78.1%, 90.4%–92.3%, and 81%–86.9%, respectively. These results are encouraging for the centers that do not have the ability to perform MRA and approximately comparable to those of the MRA study published by Schaeffeler et al.,[14] who showed a sensitivity of 82%–89%, a specificity of 87%–98%, and an accuracy of 85%–94% in detecting BP lesions. Our results highlight the ability of nonarthrographic MRI in detecting BP lesions, which is important for many centers that do not have the ability to perform MRA and depend mainly on nonarthrographic MRI for routine shoulder examination.

The classification described by Habermeyer et al.[7] was used in the current study, as we found it more convenient and easier to correlate MRI findings with those from arthroscopic examinations. Bennett's classification[5] included a detailed anatomic description of the rotator interval apex, which may not be applicable to nonarthrographic MRI examinations. Martetschläger et al. classification[2] relied on arthroscopic findings and classified BP lesions into medial sling (medial CHL/SGHL), lateral sling (lateral CHL) injuries or combined. The resolution of standard 1.5T MRI is inadequate for distinguishing between these different components.[15]

According to our arthroscopic reports, there was concordance with previous studies regarding SGHL lesions in various patient groups.[7,16] Martetschläger et al.[2] found that 36% of their patients with BP lesions had intact medial CHL/SGHL complexes with lateral CHL lesions, making them unclassifiable by Habermeyer's classification. Therefore, they suggested classifying the lesions as medial slings (medial CHL/SGHL), lateral slings (lateral CHL), or combined lesions.[2] As in previous arthroscopic studies,[7,14] Group I lesions (isolated SGHL tears) were detected in a percentage of patients in our study. A very low percentage of isolated SGHL lesions (5%) was observed by Martetschläger et al.,[2] whereas a much higher percentage (74%) was found by Bauman et al.[16] The difference in percentage between the two studies was attributed to the different inclusion and exclusion criteria.[2] The study by Bauman et al.[16] excluded all patients with full-thickness rotator cuff tears, tears >50% of the tendon thickness, and associated SLAP injuries. Our results regarding associated arthroscopically detected rotator cuff tendon lesions (Groups II, III, and IV) seem to confirm the findings of multiple previous studies[5,14,16–18] in that rotator cuff tendon injuries, specifically to their articular surfaces, are associated with biceps tendon instability. Additionally, we agree with the conclusion of Bauman et al.[16] that a BP lesion

TABLE 3. Diagnostic Value of Various MRI Signs in Detecting BP Lesions

MRI signs/Reviewer	Sensitivity	Specificity	Accuracy
SGHL discontinuity/ nonvisibility			
Reviewer 1	62.5 (20/32) [43.7–78.9]	92.3 (48/52) [81.5–97.9]	80.9 (68/84) [70.9–88.7]
Reviewer 2	56.3 (18/32) [37.7–73.6]	90.4 (47/52) [79.0–96.8]	77.4 (65/84) [66.9–85.8]
Reviewer 3	68.8 (22/32) [50.0–83.9]	92.3 (48/52) [81.5–97.9]	83.3 (70/84) [73.6–90.6]
LHB displacement on sagittal images			
Reviewer 1	65.6 (21/32) [46.8–81.4]	100 (52/52) [93.2–100.0]	86.9 (73/84) [77.8–93.3]
Reviewer 2	59.4 (19/32) [40.6–76.3]	100 (52/52) [93.2–100.0]	84.5 (66/84) [74.9–91.5]
Reviewer 3	65.6 (21/32) [46.8–81.4]	100 (52/52) [93.2–100.0]	86.9 (73/84) [77.8–93.3]
LHB subluxation/ dislocation on axial images			
Reviewer 1	37.5 (12/32) [21.1–56.3]	98.1 (51/52) [89.7–100.0]	75.0 (63/84) [64.4–83.8]
Reviewer 2	43.8 (14/32) [26.4–62.3]	100 (52/52) [93.2–100.0]	78.6 (66/84) [68.3–86.8]
Reviewer 3	43.8 (14/32) [26.4–62.3]	100 (52/52) [93.2–100.0]	78.6 (66/84) [68.3–86.8]
LHB tendinopathy			
Reviewer 1	87.5 (28/32) [71.0–96.5]	78.9 (41/52) [65.3–88.9]	82.1 (69/84) [72.3–89.7]
Reviewer 2	87.5 (28/32) [71.0–96.5]	80.8 (42/52) [67.5–90.4]	83.3 (70/84) [73.6–90.6]
Reviewer 3	87.5 (28/32) [71.0–96.5]	78.9 (41/52) [65.3–88.9]	82.1 (69/84) [72.3–89.7]
SSP tendon lesion			
Reviewer 1	59.4 (19/32) [40.6–76.3]	75.0 (39/52) [61.1–85.9]	69.0 (58/84) [58.0–78.7]
Reviewer 2	56.3 (18/32) [37.7–73.6]	75.0 (39/52) [61.1–85.9]	67.9 (57/84) [56.8–77.6]
Reviewer 3	59.4 (19/32) [40.6–76.3]	75.0 (39/52) [61.1–85.9]	69.0 (58/84) [58.0–78.7]
SSC tendon lesion			
Reviewer 1	46.9 (15/32) [29.1–64.2]	90.4 (47/52) [79.0–96.8]	73.8 (62/84) [63.0–83.8]
Reviewer 2	50.0 (16/32) [31.9–68.1]	94.2 (49/52) [84.1–98.8]	77.4 (65/84) [67.0–85.8]
Reviewer 3	50.0 (16/32) [31.9–68.1]	94.2 (49/52) [84.1–98.8]	77.4 (65/84) [67.0–85.8]

Data in parentheses were used to calculate percentages. Data in brackets are 95% confidence intervals.
BP: biceps pulley; SGHL: superior glenohumeral ligament; LHB: long head of biceps; SSP: supraspinatus; SSC: subscapularis.

is a progressive pathological process, starting with an isolated SGHL injury and finally leading to articular-side tendon tears adjacent to the rotator interval. A notable finding in our study was the considerable number of patients without SSC lesions (Groups I and II) in the BP-lesion group. Although SSC is an important stabilizing structure of the LHB, we agree with Schaeffeler et al.[14] that a normal SSC tendon does not exclude BP lesions, and vice versa. Furthermore, Godenèche et al.[19] reported intact SGHL in 25% of patients with SSC lesions.

Regarding the diagnostic value of various MRI signs for BP lesions, the LHB displacement sign showed the highest accuracy in our study, which was consistent with previous studies (74.4%–87.2%).[14,20] In contrast, Kang et al.[21] reported an accuracy of 65.6%–66.7% for the LHB displacement sign. They claimed that this relatively lower accuracy

TABLE 4. IRA for Various MRI Signs and Final MRI Diagnosis of BP Lesions

	IRA	
MRI signs	***k***	**95% CI**
SGHL discontinuity/nonvisibility	0.76	0.57–0.89
LHB displacement on sagittal images	0.93	0.85–1.00
LHB subluxation/dislocation on axial images	0.87	0.72–1.00
LHB tendinopathy	0.93	0.85–1.00
SSP tendon lesion	0.98	0.93–1.00
SSC tendon lesion	0.83	0.69–0.97
Final MRI diagnosis of BP lesions	0.78	0.64–0.93

IRA: inter-reviewer agreement; *k*: correlation coefficient; CI: confidence interval; BP: biceps pulley; SGHL: superior glenohumeral ligament; LHB: long head of biceps; SSP: supraspinatus; SSC: subscapularis.

was due to the number of patients with high-grade or full-thickness rotator cuff tears, which inferred the exact location of the LHB in relation to the SSC tendon.[21] We agree with Kang et al.[21] in that the SGHL discontinuity or nonvisibility sign has a low sensitivity but a relatively high specificity as a diagnostic sign for BP lesions. In contrast, Schaeffeler et al.[14] reported higher sensitivity and specificity for SGHL discontinuity or nonvisibility sign. Kang et al.[21] explained that rotator interval ligament evaluation might be hampered in patients with adjacent rotator cuff tendon lesions due to associated regional synovitis.

The LHB tendinopathy sign is suspected to be a consequence of chronic instability caused by BP lesions. This is an accurate sign for diagnosing BP lesions in our study and multiple other studies.[18,22,23] Multiple studies[13,14,17,20,24,25] have reported that the biceps tendon may remain within the bicipital groove, particularly in minor forms of BP lesions, which may explain the low sensitivity observed in our study and in these previous studies. However, high specificity was observed in our results, as well as in previous studies.[14,20,26]

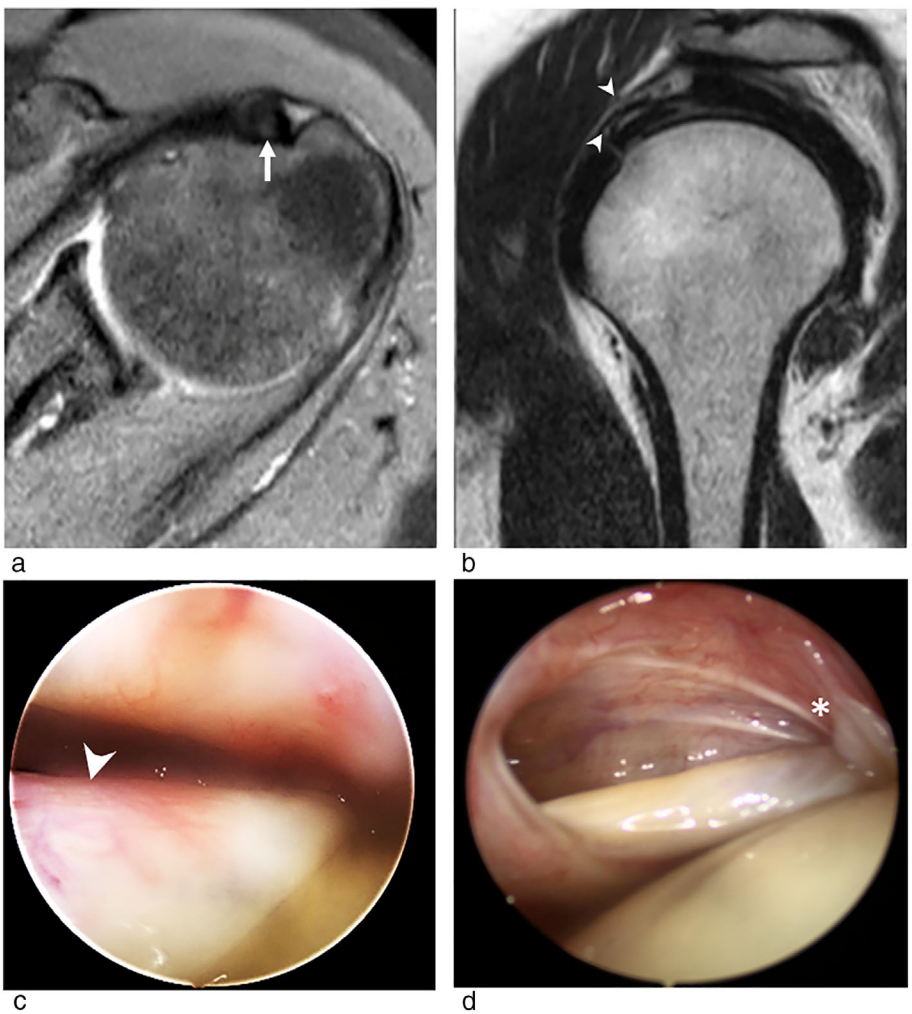

FIGURE 3: (a) Axial PDW fat-sat image shows an enlarged LHB tendon with mild signal elevation (white arrow). (b) Sagittal oblique T2WI shows intact SGHL (arrowheads). (c,d) Arthroscopic views show LHB tendinosis (arrowhead) and intact SSC tendon (asterisk). The arthroscopic report described isolated LHB tendinosis with intact BP.

FIGURE 4: (a,b) Sagittal oblique T2WI and PDW fat-sat images show nonvisible SGHL (white arrow). (c) Sagittal oblique T2WI shows caudal displacement of the LHB tendon over the SSC tendon (dashed circle). (d) Axial PDW fat-sat; centered the LHB tendon within the bicipital groove (white arrow). (e) Arthroscopic view showing torn SGHL (asterisk) and intact LHB Tendon (arrowhead). The arthroscopic report revealed a Habermeyer classification (Group I).

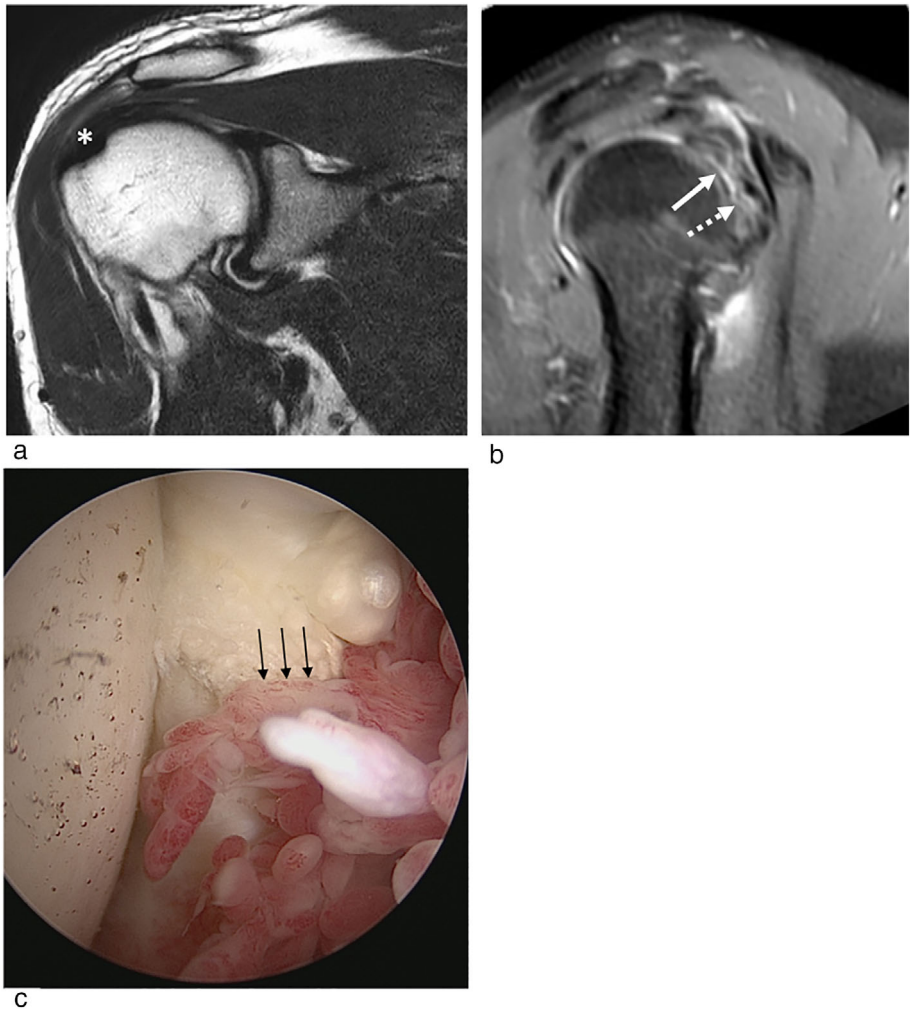

FIGURE 5: (a) Coronal oblique T2WI image shows an intact SSP tendon. (b) Sagittal oblique PDW fat-sat image shows an increased LHB tendon signal intensity (asterisk), a partial-thickness SSC tendon tear (dashed arrow), and a nonvisible intervening SGHL. (c) Arthroscopic view showing partial thickness tear of SSC tendon with associated synovial thickening (black arrows). The arthroscopic report revealed a Habermeyer classification (Group III).

Regarding SSP tendon lesions, our study found low sensitivity and moderate specificity of SSP tendon lesions for detecting BP lesions. This finding is similar to that of Schaeffeler et al.,[14] who reported low sensitivity for all readers (46%–68%); however, one reader reported a low specificity (58%), while the other two readers reported higher specificities (83% and 87%). We support the results of Schaeffeler et al.[14] regarding the use of SSC tendon lesions as a diagnostic sign for BP lesions, with low sensitivity and high specificity. In contrast, Valencia et al.[27] declared in their nonarthrographic MRI study that the BP lesions and biceps tendon instability were predictors for SSC lesions with a diagnostic accuracy of 78.8%.

In this study, as well as in Schaeffeler et al.[14] study, we excluded patients with adhesive capsulitis to provide a more precise and reliable evaluation of BP lesions in isolation and to minimize potential confounding factors that could affect the visualization of BP structures on MRI. Thickening of the anterior capsule, abnormally high signal intensity or scarring of the rotator interval, and reduced capsular distensibility in adhesive capsulitis could potentially hamper the accurate assessment of BP structures.[28] Further research on BP lesions and rotator cuff tears associated with adhesive capsulitis is encouraged.

With better evidence for the reproducibility of nonarthrographic MRI in BP diagnosis, the results of this study can be used in clinical practice. An analysis of our results demonstrated that the IRA was good regarding the final MRI diagnosis of BP lesions and was good to very good regarding various MRI signs. However, to date, no studies have assessed the IRA for such diagnostic signs using nonarthrographic MRI. Thus, our results on IRA cannot be compared with previous literature.

Limitations

This study was a monocentric retrospective study with a relatively small sample size. Many patients were not included due to the lack of detailed comments on BP structures in their

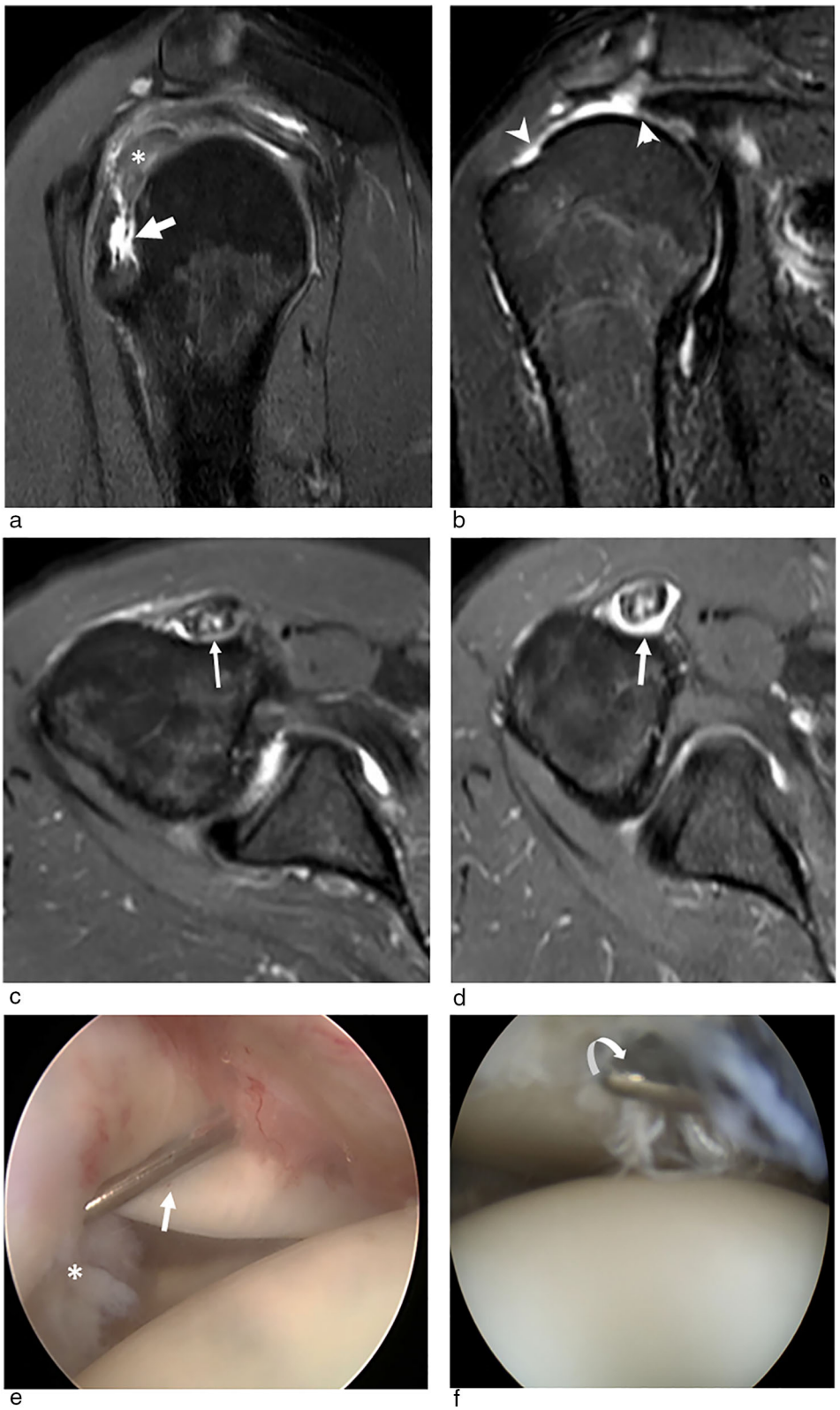

FIGURE 6: (a) Sagittal oblique PDW fat-sat image demonstrates the high signal intensity of the LHB tendon (asterisk) with adjacent partial-thickness SSC tendon tear (arrow) and torn intervening SGHL. (b) Coronal oblique PDW fat-sat image demonstrates a full-thickness SSP tear (arrowheads). (c,d) Axial PDW fat-sat images show an enlarged LHB with altered signal intensity and intrasubstance tendon tear (white arrows). (e,f) Arthroscopic views show torn SGHL (asterisk), subluxation, and tendinopathy of LHB tendon (white arrow), and full thickness SST tear (curved arrow). The arthroscopic report revealed a Habermeyer classification (Group IV).

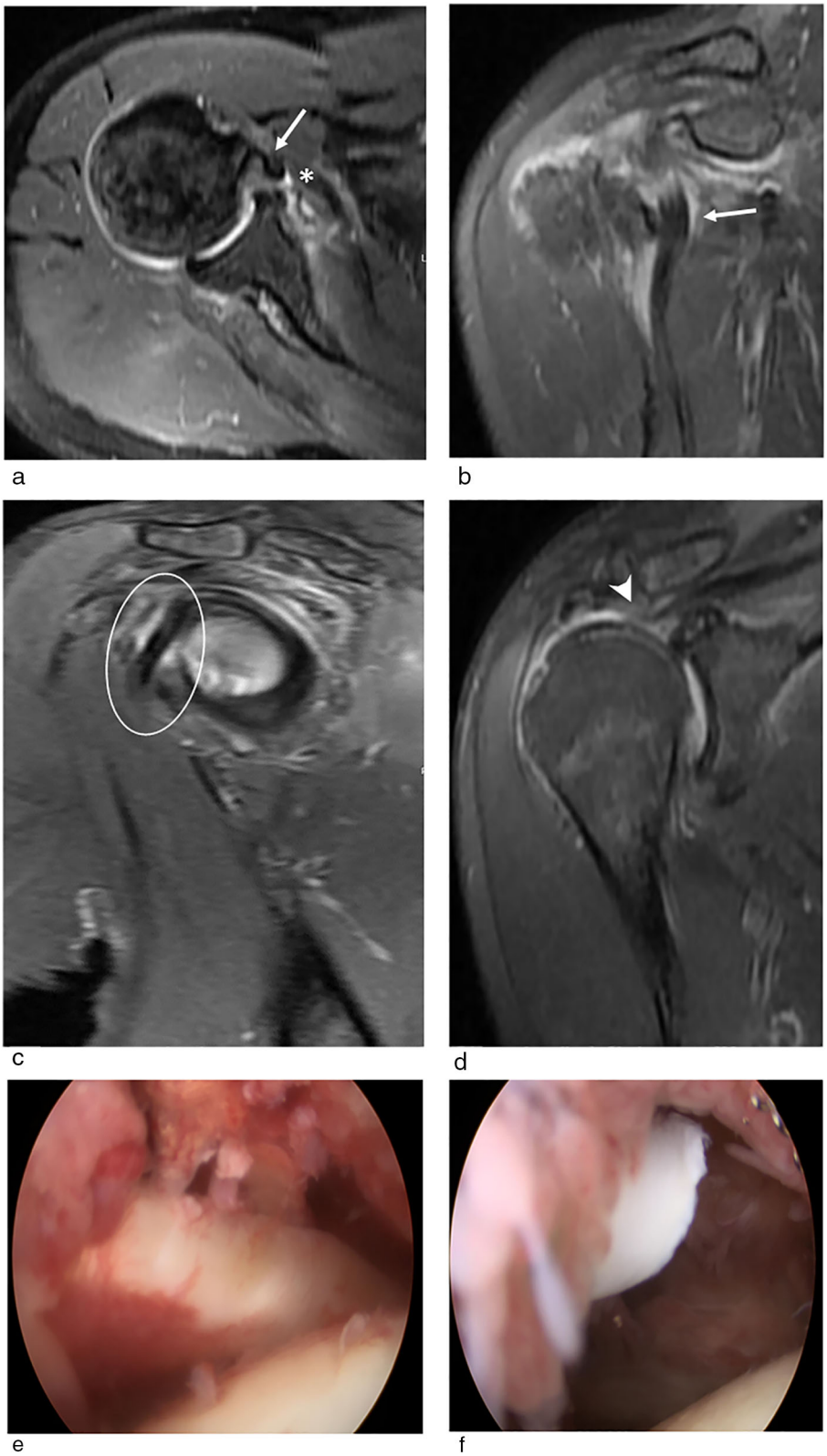

FIGURE 7: (a,b) Axial and coronal oblique PDW fat-sat image show dislocated LHB tendon with altered signal intensity (arrow) and full thickness SSC tendon tear (asterisk). (c) Sagittal oblique PDW fat-sat image shows displacement sign of LHB tendon over completely torn SSC tendon with nonvisualized intervening SGHL. (d) coronal oblique PDW fat-sat image shows a full-thickness SST tear (arrowhead). (e) Arthroscopic view shows LHB tendinopathy and sub-luxation. (f) Arthroscopic view shows full-thickness SSC tendon tear. The arthroscopic report revealed a Habermeyer classification (Group IV).

arthroscopic reports. Further prospective research with larger sample sizes and multicentric designs may be needed to validate and generalize the findings. Second, we did not evaluate CHL in our study because we followed Habermeyer's classification, which was more convenient for our nonarthrographic MRI examination, but did not consider CHL lesions. Moreover, the Habermeyer classification offers simplicity and clinical applicability, making it a more accessible and cost-effective option in daily practice. Third, the wide age range of patients may skew the results because of the natural increase of rotator cuff tears in older patients. However, the impact of age on the results may vary depending on the specific population being studied. Further research is required to better understand the relationship between age and BP lesions. Fourth, all MRI examinations were performed using a 1.5T scanner. Although higher field strengths may offer certain advantages, achieving good results with a 1.5T scanner should be seen as a positive outcome, showing the potential for future comparisons and advancements.

Conclusion

According to the results of this study, nonarthrographic shoulder MRI may have good diagnostic accuracy for detecting BP lesions. Furthermore, the LHB tendon displacement sign was the most accurate for BP lesion diagnosis, followed by the SGHL discontinuity or nonvisibility sign and the LHB tendinopathy sign.

Acknowledgment

The authors are thankful to the Deanship of Scientific Research, Najran University, Kingdom of Saudi Arabia, for funding this work under the General Research Funding program grant code NU/RG/MRC/12/1.

Author contributions

M.G.N.: Conceptualization, Data curation, Investigation, Methodology, Resources, Supervision, Validation, Visualization, Roles/Writing-original draft, Writing-review and editing. Y.E.A.: Conceptualization, Funding acquisition, Investigation, Project administration, Resources, Supervision, Validation, Visualization, Roles/Writing–original draft, Writing–review and editing. M.A.A.B.: Conceptualization, Formal analysis, Investigation, Methodology, Software, Validation, Visualization, Roles/Writing–original draft, Writing–review& editing. Y.I.L.: Formal analysis, Investigation, Methodology, Project administration, Software, Validation, Visualization, Writing-review and editing. M.M.A.Z.: Formal analysis, Investigation, Methodology, Project administration, Software, Validation, Visualization, Writing-review and editing. A.A.M.A.: Formal analysis, Investigation, Methodology, Project administration, Software, Validation, Visualization, Writing-review and editing. R.M.A.: Formal analysis, Investigation, Methodology, Project administration, Software, Validation, Visualization, Writing-review and editing. H.A.H.: Formal analysis, Investigation, Methodology, Project administration, Software, Validation, Visualization, Writing-review and editing. T.M.D.: Formal analysis, Investigation, Methodology, Validation, Visualization, Roles/Writing–original draft, Writing–review and editing. A.H.Z.: Formal analysis, Investigation, Methodology, Project administration, Software, Validation, Visualization, Writing-review and editing. S.K.A.: Conceptualization, Funding acquisition, Investigation, Project administration, Resources, Supervision, Validation, Visualization, Roles/Writing–original draft, Writing–review and editing. Y.M.A.A.Z.: Conceptualization, Data curation, Investigation, Methodology, Resources, Validation, Visualization, Writing–review and editing.

Conflict of Interests

The authors of this manuscript declare no relevant conflicts of interest, and no relationships with any companies, whose products or services may be related to the subject matter of the article.

Guarantor

The scientific guarantor of this publication is the corresponding author.

Ethical Approval

Approval was obtained from the Institutional Review Board of Zagazig University, Egypt (approval number: ZU-IRB# 9857, approved on September 26, 2022).

Informed Consent

Written informed consent was waived.

Data Availability Statement

The datasets used and/or analyzed during the current study are available from the corresponding author on reasonable request.

References

1. Nakata W, Katou S, Fujita A, Nakata M, Lefor AT, Sugimoto H. Biceps pulley: Normal anatomy and associated lesions at MR arthrography. Radiographics 2011;31(3):791-810.
2. Martetschläger F, Zampeli F, Tauber M, Habermeyer P. Lesions of the biceps pulley: A prospective study and classification update. JSES Int 2020;4(2):318-323.
3. Zappia M, Reginelli A, Russo A, et al. Long head of the biceps tendon and rotator interval. Musculoskelet Surg 2013;97(2):99-108.
4. Petchprapa CN, Beltran LS, Jazrawi LM, Kwon YW, Babb JS, Recht MP. The rotator interval: A review of anatomy, function, and normal and abnormal MRI appearance. Am J Roentgenol 2010;195(3):567-576.
5. Bennett WF. Arthroscopic repair of anterosuperior (supraspinatus/subscapularis) rotator cuff tears: A prospective cohort with 2- to 4-year follow-up. Classification of biceps subluxation/instability. Arthroscopy 2003;19(1):21-33.

6. Braun S, Horan MP, Elser F, Millett PJ. Lesions of the biceps pulley. Am J Sports Med 2011;39(4):790-795.
7. Habermeyer P, Magosch P, Pritsch M, Scheibel MT, Lichtenberg S. Anterosuperior impingement of the shoulder as a result of pulley lesions: A prospective arthroscopic study. J Shoulder Elbow Surg 2004; 13(1):5-12.
8. Szabó I, Boileau P, Walch G. The proximal biceps as a pain generator and results of tenotomy. Sports Med Arthrosc Rev 2008;16(3):180-186.
9. Bennett WF. Subscapularis, medial, and lateral head coracohumeral ligament insertion anatomy: Arthroscopic appearance and incidence of "hidden" rotator interval lesions. Arthroscopy 2001;17(2):173-180.
10. Chung CB, Dwek JR, Cho GJ, Lektrakul N, Trudell D, Resnick D. Rotator cuff interval: Evaluation with MR imaging and MR arthrography of the shoulder in 32 cadavers. J Comput Assist Tomogr 2000;24(5): 738-743.
11. Feuerriegel GC, Lenhart NS, Leonhardt Y, et al. Assessment of acute lesions of the biceps pulley in patients with traumatic shoulder dislocation using MR imaging. Diagnostics 2022;12(10):2345.
12. Lee RW, Choi SJ, Lee MH, et al. Diagnostic accuracy of 3T conventional shoulder MRI in the detection of the long head of the biceps tendon tears associated with rotator cuff tendon tears. Skeletal Radiol 2016;45(12):1705-1715.
13. Malavolta EA, Assunção JH, Guglielmetti CL, de Souza FF, Gracitelli ME, Neto AA. Accuracy of preoperative MRI in the diagnosis of disorders of the long head of the biceps tendon. Eur J Radiol 2015; 84(11):2250-2254.
14. Schaeffeler C, Waldt S, Holzapfel K, et al. Lesions of the biceps pulley: Diagnostic accuracy of MR arthrography of the shoulder and evaluation of previously described and new diagnostic signs. Radiology 2012; 264(2):504-513.
15. Feuerriegel GC, Neumann J, Wurm M, Comment on "Feuerriegel et al. Assessment of acute lesions of the biceps pulley in patients with traumatic shoulder dislocation using MR imaging. Diagnostics 2022;12(10): 2345.
16. Baumann B, Genning K, Böhm D, Rolf O, Gohlke F. Arthroscopic prevalence of pulley lesions in 1007 consecutive patients. J Shoulder Elbow Surg 2008;17(1):14-20.
17. De Maeseneer M, Boulet C, Pouliart N, et al. Assessment of the long head of the biceps tendon of the shoulder with 3T magnetic resonance arthrography and CT arthrography. Eur J Radiol 2012;81(5):839-934.
18. Weishaupt D, Zanetti M, Tanner A, Gerber C, Hodler J. Lesions of the reflection pulley of the long biceps tendon MR arthrographic findings. Invest Radiol 1999;34(7):463-469.
19. Godenèche A, Nové-Josserand L, Audebert S, et al. Relationship between subscapularis tears and injuries to the biceps pulley. Knee Surg Sports Traumatol Arthrosc 2017;25(7):2114-2120.
20. Zappia M, Ascione F, Di Pietto F, et al. Long head biceps tendon instability: Diagnostic performance of known and new MRI diagnostic signs. Skeletal Radiol 2021;50(9):1863-1871.
21. Kang Y, Lee JW, Ahn JM, Lee E, Kang HS. Instability of the long head of the biceps tendon in patients with rotator cuff tear: Evaluation on magnetic resonance arthrography of the shoulder with arthroscopic correlation. Skeletal Radiol 2017;46(10):1335-1342.
22. Zanetti M, Weishaupt D, Gerber C, Hodler J. Tendinopathy and rupture of the tendon of the long head of the biceps brachii muscle: Evaluation with MR arthrography. AJR Am J Roentgenol 1998;170(6): 1557-1561.
23. Buck FM, Grehn H, Hilbe M, Pfirrmann CW, Manzanell S, Hodler J. Degeneration of the long biceps tendon: Comparison of MRI with gross anatomy and histology. AJR Am J Roentgenol 2009;193(5):1367-1375.
24. Spritzer CE, Collins AJ, Cooperman A, Speer KP. Assessment of instability of the long head of the biceps tendon by MRI. Skeletal Radiol 2001;30(4):199-207.
25. Baptista E, Malavolta EA, Gracitelli MEC, et al. Diagnostic accuracy of MRI for detection of tears and instability of proximal long head of biceps tendon: An evaluation of 100 shoulders compared with arthroscopy. Skeletal Radiol 2019;48(11):1723-1733.
26. Buck FM, Dietrich TJ, Resnick D, Jost B, Pfirrmann CW. Long biceps tendon: Normal position, shape, and orientation in its groove in neutral position and external and internal rotation. Radiology 2011;261(3): 872-881.
27. Valencia REA, Miguel LAC, Ruiz SM. Diagnostic correlation of simple magnetic resonance imaging and shoulder arthroscopy for long head of the biceps instability as a predictor of subscapularis injury. Acta Med Austriaca 2022;20(4):317-322.
28. Zappia M, Di Pietto F, Aliprandi A, et al. Multi-modal imaging of adhesive capsulitis of the shoulder. Insights Imaging 2016;7(3):365-371.